Acta Pharmaceutica Sinica B 2024;14(2):808–820

Chinese Pharmaceutical Association
Institute of Materia Medica, Chinese Academy of Medical Sciences

Acta Pharmaceutica Sinica B

www.elsevier.com/locate/apsb
www.sciencedirect.com

ORIGINAL ARTICLE

mIgM-mediated splenic marginal zone B cells targeting of folic acid for immunological evasion

Huan Wang[a,b,†], Zhuxuan Jiang[a,†], Zhiwei Guo[a,c,†], Gan Luo[a], Tianhao Ding[a], Changyou Zhan[a,c,*]

[a]*Department of Pharmacology, School of Basic Medical Sciences & Department of Pharmacy, Shanghai Pudong Hospital, Fudan University, Shanghai 200032, China*
[b]*Department of Pharmaceutical Sciences, School of Pharmacy, Naval Medical University, Shanghai 200433, China*
[c]*Shanghai Engineering Research Center for Synthetic Immunology, Fudan University, Shanghai 200032, China*

Received 9 June 2023; received in revised form 14 August 2023; accepted 28 August 2023

KEY WORDS

Membrane-bound IgM;
Anti-drug antibodies;
B cell anergy;
Folic acid;
Marginal zone B cells;
B cell receptor;
Biologics;
Targeting

Abstract Folic acid is a fully oxidized synthetic folate with high bioavailability and stability which has been extensively prescribed to prevent congenital disabilities. Here we revealed the immunosuppressive effect of folic acid by targeting splenic marginal zone B (MZB) cells. Folic acid demonstrates avid binding with the Fc domain of immunoglobulin M (IgM), targeting IgM positive MZB cells *in vivo* to destabilize IgM-B cell receptor (BCR) complex and block immune responses. The induced anergy of MZB cells by folic acid provides an immunological escaping window for antigens. Covalent conjugation of folic acid with therapeutic proteins and antibodies induces immunological evasion to mitigate the production of anti-drug antibodies, which is a major obstacle to the long-term treatment of biologics by reducing curative effects and/or causing adverse reactions. Folic acid acts as a safe and effective immunosuppressant *via* IgM-mediated MZB cells targeting to boost the clinical outcomes of biologics by inhibiting the production of anti-drug antibodies, and also holds the potential to treat other indications that adverse immune responses need to be transiently shut off.

*Corresponding author.
E-mail address: cyzhan@fudan.edu.cn (Changyou Zhan).
[†]These authors made equal contributions to this work.
Peer review under the responsibility of Chinese Pharmaceutical Association and Institute of Materia Medica, Chinese Academy of Medical Sciences.

https://doi.org/10.1016/j.apsb.2023.09.011

1. Introduction

Therapeutic biologics have become overwhelming to significantly improve clinical outcomes for patients with intractable diseases (*e.g.,* cancers, autoimmune diseases, and inflammatory diseases)[1−3]. However, biologics such as therapeutic proteins, monoclonal antibodies, gene therapies and vaccines are generally immunogenic to stimulate immune systems for production of anti-drug antibodies (ADAs) after long-term treatments[4]. Unwanted ADAs of biologics reduce the therapeutic potency *via* interference with epitope binding and/or formation of immune complexes, accelerating blood clearance and even inducing adverse reactions[5]. For example, a very high incidence of ADAs (ranging 20%−70%) was observed in the clinical studies of adalimumab and its biosimilars in healthy volunteers[6]. ADAs remain a major obstacle to the clinical application of biologics. Animal and clinical studies have revealed that immunogenicity shares both T-cell-dependent (requirement of $CD4^+$ T cells) and T-cell-independent (involvement of MZB cells) characteristics[7].

B cell anergy is important in preventing the development of antibody responses to protein antigens. Anergy is a state where B cells exist unresponsiveness in the periphery with the possibility of reversal. Cells bearing desensitized receptors remain capable of binding antigens, but are unable to transduce signals. Anergic B cells do not proliferate following B cell receptor (BCR) ligation[8−11]. The mIgM-BCR complex consists of monomeric membrane-bound IgM (mIgM) that forms the antigen-binding molecule, which is non-covalently associated with the signal-transduction unit composed of a heterodimer of the immunoglobulin α-chain (Igα) and immunoglobulin β-chain (Igβ)[12]. Splenic MZB cells harboring a large number of mIgM-BCR strategically locate in response to blood-borne antigens and rapidly differentiate into antibody-producing plasma cells in red pulp[13,14]. MZB cells are thus an important target to regulate the immune response of the body.

Folic acid (FA) is a fully oxidized synthetic folate (pteroylmonoglutamic acid) with high bioavailability and stability. As a small-molecule ligand of folate receptors with high affinity, FA becomes a star molecule in basic research and pharmaceutical industry to facilitate cancer targeting[15,16]. Even though laborious efforts have been made to promote the clinical translation of FA-enabled cancer targeting, few achievements have been made to date[17,18]. We recently found that secreted IgM (sIgM) in blood heavily absorbs on the surface of FA functionalized liposomes, accelerating liposome clearance and inducing the immune response[19,20]. This discovery makes us reflect on the targeting of FA-functionalized nanomedicines and pay attention to the interaction between FA and mIgM, which has a monomer molecular structure similar to sIgM.

In this study, we discover avid binding of FA with the Fc domain of IgM which redirects FA to target splenic MZB cells. FA can induce B-cell anergy *via* destabilizing mIgM-BCR complex to interfere with immune response. Covalent conjugation of FA with immunogens or therapeutics induces immunological evasion to at least partially mitigate the production of ADAs.

2. Materials and methods

2.1. Regents and antibodies

FA-PEG-Cy5, PEG-Cy5 and FA-conjugated ovalbumin (FA-OVA, FA/OVA at a molar ratio of 23:1) were purchased from Xi'an Ruixi Biological Technology Co., Ltd. (Xi'an, China). $mPEG_{2000}$-DSPE (methoxyl-polyethylene $glycol_{2000}$-1,2-distearoyl-*sn*-glycero-3-phosphoethanolamine) was purchased from AVT Pharmaceutical Technology Co., Ltd. (Shanghai, China). Ovalbumin was purchased from Siama. CD79B (D7V2F) rabbit mAb (#96024) was from Cell Signaling Technology (Boston, MA, USA). CD79A (HM47, sc-200640) was from Santa Cruz biotechnology, Inc. (Santa Cruz, CA, USA). Goat-anti-mouse IgM (115-005-075), fluorescein-conjugated donkey anti-mouse IgM (715-095-140) and F $(ab')_2$ goat anti-mouse IgM (115-006-020) were from Jackson ImmunoResearch Laboratories (West Grove, PA, USA). PE conjugated rat anti-mouse CD19 (553786), PE rat anti-mouse CD86 (561963), and APC rat anti-mouse CD19 (550992) were from BD Pharmingen (San Diego, CA, USA). FITC anti-mouse/human GL7 antigen (GL7), PE anti-mouse CD21/CD35 (7E9), PE/Cyanine7 anti-mouse CD23 (B3N4), PE anti-mouse CD11c (N418), PE anti-mouse F4/80 (BM8), PE anti-mouse CD68 (FA-11), purified anti-mouse IgE (RME-1) and anti-mouse IgA (RMA-1) were acquired from BioLegend (San Diego, CA, USA). HRP conjugated goat anti-mouse IgM mu chain (ab97230), HRP conjugated goat anti-rat IgM mu chain (ab97180), HRP conjugated goat anti-monkey IgG (ab112767), HRP conjugated goat anti-monkey IgG2a (ab97245), HRP conjugated goat anti-monkey IgG1 (ab97240), HRP conjugated goat anti-human IgG (ab97205), recombinant human folate binding protein (ab167698), HRP conjugated anti-6X His tag antibody (ab1187), normal mouse IgM (ab18400), and normal mouse IgG (ab188776) were from Abcam (Cambridge, MA). APC anti-mouse IgM (17-5790-82) were purchased from Thermo Fisher Scientific (Shanghai, China). PE anti-mouse IgG1 Antibody were acquired from Biolegend (San Diego, CA, USA). Antibody against GAPDH (TA-08) was from Zhongshan Golden Bridge (Beijing, China). Antibody against DDDDK-tag (AP0007) and mouse IgG (BD0050) was from BioWorld Biotechnology (Minneapolis, MN, USA). Tyrosine phosphate-specific mAb (4G10) was obtained from Merck (Darmstadt, Germany). Adalimumab (Humira, AbbVie), infliximab (Remicade, Cilag AG), human Coagulation Factor hFVIII (Hemoraas, Shanghai RAAS Blood Products) and recombinant human interferon alfa-2b (Kayinyisheng, Beijing Kawin) were acquired from Huashan Hospital, Fudan University, China.

2.2. Cell lines, animals and human serum

Human lymphoma BJAB cell line was purchased from the Type Culture Collection of Chinese Academy of Sciences (Shanghai, China). Adult male ICR mice, BALB/c mice, C57BL/6J, severe combined immunodeficient (SCID) mice, and Sprague−Dawley (SD) rats at the age of 6−8 weeks were acquired from Shanghai SLAC Laboratory Animal Co., Ltd. (Shanghai, China). FVIII-deficient mice (C57BL/6J background) were obtained from Beijing Biocytogen Co., Ltd. All animals were kept under SPF condition and animal procedures were performed in accordance with the Guidelines of the Care and Use of Laboratory Animals of Fudan University and approved by the Animal Ethics Committee of Fudan University. Lymphocyte suspensions were isolated from spleen or lymph nodes of BALB/c mice using lymphocyte separation medium following the manufacturer's instruction (DKW33-R0100, Dakwei Biotechnology Co., Ltd., China). The use of human serum in the present work was approved the Ethics Committee of the Fudan University and informed consent was collected from donors.

2.3. ELISA

Direct binding of FA with natural immunoglobulins was investigated using ELISA assay. Two micrograms of 1,2-distearoyl-*sn*-glycero-3-phosphoethanolamine-*N*-[methoxy-(polyethyleneglycol)-2000] (PEG-DSPE) or FA-PEG-DSPE was coated on 96-well ELISA plates overnight, rinsed with PBS and blocked with 5% bovine serum albumin (BSA) for 1 h. Serial dilutions of serum (diluent solvent was PBS or PB with 0.75 mol/L sodium chloride) were added and incubated for 1 h at 37 °C. After three rinses with PBS and blocking with 3% BSA, the corresponding horseradish peroxidase conjugated antibody (*e.g.*, anti-IgM) was added and incubated for 1 h. After 15 min reaction with 3,3',5,5-Tetramethylbenzidine (TMB) and termination with sulfuric acid (0.18 mol/L), absorbance at 450 nmol/L was measured using a multifunctional plate reader (Tecan Spark, Switzerland). For competitive binding of FA, diluted serum of BALB/c mice (1:8) were pre-incubated with serial dilutions of free FA (dissolved in deionized water containing 0.075 mol/L sodium chloride and 0.075 mol/L sodium bicarbonate solution, pH 7.4) for 0.5 h at 37 °C. As for the evaluation of binding kinetics, diluted serum of BALB/c mice (1:4) was added at the predominated time points to investigate the effect of incubation duration on natural IgM binding. As for effect of different IgM origin, serum from SD rats, cynomolgus monkey and healthy volunteer were used. Then serum was added into FA-PEG-DSPE coated 96-well ELISA plates and incubated for 1 h at 37 °C, followed by treating as aforementioned.

2.4. Molecular modeling

The 3D structures of mIgM and mIgα/β were extracted from the cryo-EM structure of mIgM-mIgα/β (PDB code: 7XQ8) for subsequent molecular modelling. The possible ligand-binding pockets were detected by using Fpocket program, and the molecular docking between FA and mIgM was performed *via* Maestro. The docking pose of FA-mIgM was inserted into a preequilibrated 1,2-dioleoyl-*sn*-glycero-3-phosphocholine (DOPC) bilayer by using the Membrane Builder module in the CHARMM-GUI program. The chemical structure of FA was created by Chem3D, was then optimized, and the partial atomic charges were calculated by AM1-BCC method *via* Antechamber module in AMBER20 to obtain the molecular mechanics parameters of FA. Subsequently, the molecular mechanics parameters from ff19SB and GAFF force field were assigned to the docking pose of FA-mIgM which were then neutralized by adding sodium/chlorine counter ions and solvated in a cuboid box of transferable interatomic potential with three points model (TIP3P) water molecules with solvent layers 12.0 Å between solute surface and box edges, *via* LEaP module in AMBER20. According to box size, specific counts of sodium/chlorine ions were added to achieve the 150 mmol/L NaCl at system. Molecular dynamics (MD) simulation was conducted by using AMBER20. The SHAKE algorithm was employed to constrain all covalent bonds involving hydrogen atoms. Energy minimization was performed *via* pmemd.MPI module. Solvent and ions were optimized by 10000 steps of steepest descent minimization (NPT) with protein backbone restrained by 10 kcal/mol$Å^2$. Then, NVT minimization containing 5000 steps of steepest descent minimization and 5000 steps of conjugated gradient minimization was respectively applied to the system with protein backbone restrained by 10 kcal/mol$Å^2$ and backbone Cα atoms restrained by 5 kcal/mol$Å^2$. Last, the system was fully relaxed by 20000-step steepest descent and 20000-step conjugated gradient minimizations without any restraint to remove unfavorable contacts. Subsequently, the system was gradually heated from 0 to 100 K in 40 ps with a time step of 0.5 fs, and maintained 100 K for 10 ps. The system was then heated from 100 to 300 K in 160 ps with a time step of 2 fs and maintained 300 K for 40 ps, by using Langevin dynamics at a constant volume. A 200-ps density equilibration was conducted to optimize the heated system that was subsequently undergone two steps of NPT ($T = 300$ K, $P = 1$ atm) equilibration with or without restrain for total 200 ps. Finally, the system was submitted to a 100-ns NPT ($T = 300$ K, $P = 1$ atm) production MD simulation by pmemd.cuda module. MD trajectory was analyzed by using CPPTRAJ, and the RMSD and radius of gyration were thus calculated. 2D free energy landscape was clustered and mapped by Gromacs 2022.1. Molecular docking between mIgM and mIgα/β was performed by Maestro. The cryo-EM structure and simulated structure of mIgM-mIgα/β were fully relaxed by Rosetta platform, and generated three optimized structures per complex. The binding free energy between mIgM and mIgα/β was calculated by using Hawkdock MM/GBSA module. All 3D structures involved in this study were visualized by PyMOL.

2.5. Biodistribution

BALB/c mice were intravenously injected with FA-PEG-Cy5 or PEG-Cy5 (5 nmol per gram of mice). Mice were sacrificed 1 h and 4 h after injection. Blood was sampled, and liver, spleen and lung were collected, weighed and homogenized with 5% triton-X 100. Fluorescence intensity of plasma and tissue extractions were detected by a fluorescence spectrophotometer ($E_x = 550$ nm, $E_m = 570$ nm, Tecan Spark, Switzerland). To observe the distribution of FA-PEG-Cy5, spleen was dissected at 1 h after injection, frozen sectioned, and stained with DAPI and antibodies to identify co-localization with $CD19^+$ B lymphocytes, IgM^{hi} MZB cells for microscopic observation using a laser scanning confocal microscope (TCS SP5, Leica, Germany).

2.6. Cellular binding

To evaluate the binding of FA with mIgM, splenic lymphocytes, BJAB cells and transfected cell line were incubated with FA-PEG-Cy5 (10 μmol/L) or PEG-Cy5 at 4 °C overnight. Cells were stained with DAPI and fluorescein-labeled anti-IgM antibody (715-095-140, Jackson) then visualized using a laser scanning confocal microscope (TCS SP5, Leica, Germany). Anti-IgM antibody (ab97230) was utilized to deplete the mIgM on B lymphocytes after 12 h of incubation at 37 °C. Binding affinity of FA-PEG-Cy5 with B lymphocytes (gated as $CD19^+$) was quantified by a flow cytometer (FACS Aria, BD). Binding affinity of FA-PEG-Cy5 with 293T cells expressing mIgM-BCR was quantified by a flow cytometer (FACS Aria, BD).

2.7. Free folic acid determination in serum

Free FA was measured by ultrafiltration after incubation with serum. The equal volume of serum (ICR mouse, SCID mouse, and SCID mouse plus 50 μg/mL of IgM or IgG) and folic acid solution were mixed and incubated at 37 °C for 1 h, then centrifuged at 10,000 × *g* for 60 min in an ultrafiltration tube (MWCO 3 kDa). Free folic acid in the filtrate was measured using reversed-phase high performance liquid chromatography (HPLC) under the

following conditions: 40 °C, C18 column (YMC, 3.5 μm, 4.6 × 150 mm), 5% acetonitrile in 0.05M KH_2PO_4 solution (pH 6.3) at a flow rate of 0.6 mL/min, and UV absorbance at 285 nm.

2.8. Mice immunization with OVA

BALB/c mice were intravenously immunized with 10 μg of OVA, FA-OVA, mixture solution of FA and OVA or saline weekly for 3 weeks. All mice were boosted with 10 μg of OVA on Days 21, 28 and 35. Mice were bled on the predetermined time points and serum were collected. OVA-specific IgG and IgE levels were quantitated using ELISA. Briefly, 96-well plates were coated with OVA (5 μg per well) for overnight, incubated with diluted serum samples and then applied with horseradish peroxidase-conjugated secondary anti-mice antibodies. Body temperature was recorded after each OVA boost at a 15 min interval. Spleen was harvested at 4 h after the first OVA boost on Day 21 for frozen sectioning. After IgM and DAPI staining, the slices were visualized using a laser scanning confocal microscope. On Day 21, splenic lymphocytes were isolated for phenotype analysis. Cells were incubated with anti-CD19, anti-CD86 and anti-GL7 antibodies to analysis the proliferation and differentiation levels of B lymphocytes.

2.9. Plasmid and cell transfection

The plasmid mIg heavy chain μ and mIg light chain λ were kind gifts from Dr. Wang Jiyang (Fudan University, shanghai, China). Plasmids encoding mouse Igα/Igβ were all constructed in pcDNA3.1-3 × Flag-C backbone. 293T cell was purchased from the Type Culture Collection of Chinese Academy of Sciences (Shanghai, China) and maintained in Dulbecco's modified Eagle medium with 10% fetal bovine serum (FBS), 100 μg/mL penicillin and 100 μg/mL streptomycin. The A20 B lymphoma cells was purchased from the Type Culture Collection of Chinese Academy of Sciences (Shanghai, China) and maintained in complete RPMI-1640 medium with 10% fetal bovine serum (FBS), 100 μg/mL penicillin and 100 μg/mL streptomycin (Invitrogen). All cells were maintained in an incubator containing 5% CO_2 at 37 °C. 293T cells or A20 cells were co-transfected with plasmid pμ, pλ, pIgα and pIgβ by Lipofectamine 2000 (Invitrogen, Carlsbad, CA) or electroporation (Lonza), respectively. Transfection efficiency was evaluated by flow cytometry.

2.10. Immunoprecipitation and detection of tyrosine phosphorylated proteins in vitro

Transfected cell lines were incubated with FA at indicated dose for 6 h at 37 °C in the absence or presence of crosslinking anti-IgM antibody (10 μg/mL) for the indicated time afterwards. Cells were lysated in lysis buffer containing phosphatase inhibitor cocktail (ab201112, Abcam) and protease inhibitor (04693116001, Roche) and hold on ice for 30 min. Supernatant was collected by centrifugation at 12,000 × g for 10 min. Lysates were adjusted to the same protein concentration using BCA protein assay kits. The whole-cell lysates were separated by SDS-polyacrylamide gel electrophoresis and electrotransferred to polyvinylidene difluoride membrane to detect total tyrosine phosphorylation proteins by mAb 4G10. Anti-μ antibody (115-005-075, Jackson) used for immunoprecipitation was incubated with lysates at 4 °C overnight according to the manufacturer's instruction (Abs955, Absin). Then immunoprecipitate was fractionated using 12% SDS-PAGE gels. The separated protein was transferred to polyvinylidene difluoride membranes for immunoblotting assay. Combination of mIgM and Igα/β were detected using respective antibodies.

2.11. Ca^{2+} mobilization analysis

Intracellular Ca^{2+} mobilization of A20 cells expressing mIgM-BCR were monitored by processed with Rhod-2/AM and 0.02% Pluronic F127 (Yeasen Biotechnology, Shanghai, China) at 30 °C for 30 min in HBSS buffer. Then cells were incubated at 37 °C for 15 min in HBSS buffer. Treated cells were stimulated with anti-IgM Fab, calcium flux was measured by flow cytometry.

2.12. FA-conjugation

For antibody conjugation, adalimumab and infliximab were partially reduced by 1 mmol/L equivalents tris(2-carboxyethyl) phosphine hydrochloride (TECP) and 5 mmol/L EDTA in PBS at room temperature for 90 min. Then, reduced adalimumab and infliximab were alkylated with 30 molar equivalents of FA-PEG400-MAL for 20 min at room temperature. The reaction mixtures were then loaded into 3.5K MWCO dialysis cassettes and dialyzed with PBS for 72 h. The molar ratio of FA to antibodies were determined by quantifying FA using spectrophotometry (Cary 60 UV−Vis, Aglient Technologies, CA) at 370 nm, and antibodies by BCA protein assay kits (Thermo Scientific, MA). Adalimumab and Infliximab yielded average FA conjugating ratios of 1:5.6 and 1:3.6, respectively.

Folic acid conjugated hFVIII and interferon α2b were prepared as follows. In brief, excess folic acid (360 molar equivalents for hFVIII and 30 molar equivalents for interferon α2b) was reacted with 1-ethyl-3-(3-dimethylaminopropyl)-carbodiimide (EDC) at a molar ratio of 0.6:1, and then added to 0.1 mol/L sodium carbonate buffer protein solution (pH 9.5). The mixture was maintained at pH 6.6 overnight. Folic acid conjugated hFVIII and interferon α2b were then loaded into 3.5 kDa MWCO dialysis cassettes against PBS for 72 h. Folic acid was quantified using spectrophotometry (Cary 60 UV−Vis, Aglient Technologies, CA) at 370 nm, and proteins were quantified by BCA protein assay kits (Thermo Scientific, MA). hFVIII and interferon α2b yielded average FA conjugating ratios of 1:34.8 and 1:1.5.

2.13. Mice immunization with biologics

Mice were randomly divided into three groups for each tested biologic. In the first group, BALB/c mice were weekly administered with adalimumab (3 mg/kg, s.c.), infliximab (6 mg/kg, i.v.) or interferon α2b (4 × 10^6 IU, s.c.). In the second group, mice were weekly immunized with folic acid conjugated biologics with equivalent dose. In the third group, mice were intragastrically administered with 150 mg/kg folic acid apart from weekly immunization with biologics.

Similar to BALB/c mice, FVIII-deficient mice were also divided into 3 groups, and weekly treated with 80 IU/kg of hFVIII, hFVIII conjugated with folic acid, and hFVIII combined with folic acid intragastric administration.

2.14. ADA detection

For three groups of mice weekly immunized with each biologic, serum samples were collected at different weeks: 4 weeks for BALB/c mice treated with adalimumab and infliximab, 8 weeks

for mice treated with interferon α2b, and 3 weeks for FVIII-deficient mice treated with hFVIII. Since interferon α2b induced very low ADA level at the 4th week, mice were weekly stimulated with interferon α2b for the 8 weeks. ADA levels of specific IgG were then measured by ELISA. Plates were coated with biologics antigens (2 μg of adalimumab, 2 μg of infliximab, 0.025 IU of hFVIII, or 5×10^4 IU of interferon α2b each well) overnight. The plates were then blocked with 3% BSA, incubated with diluted serum samples, applied with Anti-mice IgG antibodies conjugated with horseradish peroxidase, and processed with same protocols as ELISA experiments described above. Specific serum IgG titer was identified as the Log serum dilution for OD_{450} of tested group to be equal to 2.1-fold OD_{450} of PBS group, and the calculation was accomplished by Graphpad 8.02 software using four-parameter nonlinear regression.

2.15. *Bleeding assays*

After two weekly immunizations, all 3 groups of FVIII-deficient mice were administered with 80 IU/kg hFVIII by tail intravenous injection. One hour later, mice were anesthetized with chloral hydrate and laid in supine position. The distal 3 mm of mice tails were then transected and immersed into 37 °C 15 mL saline for 20 min. The obtained saline samples containing blood were then treated with red blood cell lysis buffer (155 mmol/L NH_4Cl, 10 mmol/L $KHCO_3$, 0.1 mmol/L Na_2EDTA, pH = 7.3) to lyse red blood cells. The sample absorbance was then measured at 405 nmol/L to calculate blood loss volume, while standard curve was established by WT C57BL/6J mice blood with identical treatment.

2.16. *Statistical analysis*

Data are mean ± standard deviations (SDs) and analyzed by Student's *t*-test or ANOVA with GraphPad Prism software 6.0.4. $P < 0.05$ was considered statistically significant (n.s. indicates $P > 0.05$, $0.01 <^{*} P < 0.05$, $0.001 <^{**} P < 0.01$, $^{***}P < 0.001$).

3. Results

3.1. *Folic acid specifically binds mIgM*

Our recent work revealed that FA-conjugated liposomes massively absorbed sIgM, leading to deprivation of FA targeting activity and rapid blood clearance and heavy hepatic accumulation of liposomes *in vivo*[19,20]. In the direct binding assay (see Methods), FA interacted with mouse sIgM in a concentration-dependent manner, registering an estimated equilibrium constant (K_d) value of 12 nmol/L (Fig. 1A). Natural IgM was previously identified to bind a positively charged brain targeting peptide ^{D}CDX mainly *via* electrostatic interaction, which could be impaired by adding high concentration of sodium chloride (0.75 mol/L, Supporting Information Fig. S1). In contrast, the specific binding of FA with sIgM could be competitively inhibited by free FA (Fig. 1B) but not concentrated salt (Fig. 1C), excluding the electrostatic interaction between FA and sIgM. The binding of FA with mouse sIgM was fast, which plateaued within 30 min (Fig. 1D). The other classes of mouse secretory immunoglobulins, including IgG, IgA and IgE, exhibited undetectable binding with FA (Fig. 1E). sIgM from other species and human also demonstrated avid binding with FA (Fig. 1F).

mIgM that constitutes the BCR possesses an identical amino acid sequence with sIgM except for an extension in constant μ4 (Cμ4) region at the 3′-end[12,21], and thus mIgM may bond FA in the same mode as sIgM. Despite avid binding with sIgM, approximate 50% of FA was free in blood (Supporting Information Fig. S2), suggesting the accessibility of FA to mIgM *in vivo*. FA-PEG-Cy5 (FA covalently linked to the fluorescent dye Cy5 with a polyethylene glycol 2000 spacer) was further used to investigate binding with mIgM. After overnight incubation at 4 °C, FA-PEG-Cy5 exhibited significant binding with mouse splenic B lymphocytes and colocalization with mIgM (Fig. 1G). Meanwhile, FA-PEG-Cy5 binding with splenic B lymphocytes depended on the mIgM expression level. mIgM exhaustion by anti-IgM antibody effectively inhibited splenic B lymphocytes binding FA-PEG-Cy5 (Fig. 1H). Effective binding of FA with human mIgM was also observed after overnight incubation with BJAB cells (human derived $mIgM^+$ Burkitt lymphoma) at 4 °C (Supporting Information Fig. S3).

3.2. *Folic acid targets splenic marginal zone B cells* via *mIgM*

The *in vivo* biodistribution of FA-PEG-Cy5 was quantified in BALB/c mice at 1 and 4 h after intravenous injection (Fig. 2A and B). In blood, FA-PEG-Cy5 exhibited higher residual concentrations in blood than PEG-Cy5 at both time points. FA-PEG-Cy5 displayed higher accumulation in kidney as expected than PEG-Cy5 due to the overexpression of folate receptors (Supporting Information Fig. S4). In spleen, both FA-PEG-Cy5 and PEG-Cy5 were mainly accumulated in the red pulp (Fig. 2C). FA-PEG-Cy5 exhibited significantly higher uptake by MZB cells than PEG-Cy5, and colocalized well with mIgM (Fig. 2D). MZB cells were further sorted by gating the $CD19^+CD21^{hi}CD23^{lo}$ subgroup of splenic B lymphocytes using flow cytometry. The results showed that FA conjugation induced a 3-fold increase of the mean Cy5 fluorescence intensity in MZB cells (Fig. 2E). To analyze the correlation between mIgM expression and FA-PEG-Cy5 uptake, splenic B lymphocytes were divided into three subgroups according to the mIgM expression levels (Fig. 2F). The uptake of FA-PEG-Cy5 was positively correlated with the expression level of mIgM. To study if folate receptors (FRs) contribute to FA targeting, the mRNA transcript levels of *FOLR1* and *FOLR2* were analyzed using quantitative RT-PCR (Supporting Information Fig. S4A and S4B). Both *FOLR1* and *FOLR2* demonstrated low expression levels in all organs except kidney. Low expression of FRs in spleen was also convinced by Western blot assay (Fig. S4C), excluding the implication of FRs in MZB cells targeting. In addition, splenic B lymphocytes binding of FA could not be significantly inhibited by anti-complement receptors antibody or complement inactivation (see Methods, Supporting Information Fig. S5), validating mIgM as the main receptor for FA targeting.

The uptake of FA-PEG-Cy5 by other splenic antigen presenting cells (APCs) was analyzed after staining with corresponding antibodies (Supporting Information Fig. S6). No significant targeting of FA-PEG-Cy5 was observed with splenic dendritic cells. The calculated Pearson's *R* values of FA-PEG-Cy5 and PEG-Cy5 with splenic dendritic cells were respective 0.12 and 0.10. Similar situation was in the uptake of FA-PEG-Cy5 by splenic resident macrophages. There was also no significant targeting of FA-PEG-Cy5 in lymph node B lymphocytes or dendritic cells (Supporting Information Figs. S7 and S8) *via* tail vein injection.

3.3. *Folic acid reversibly suppresses the humoral immunity*

To investigate the FA-induced immunological response *via* MZB targeting, FA conjugated ovalbumin (FA-OVA, with an average FA

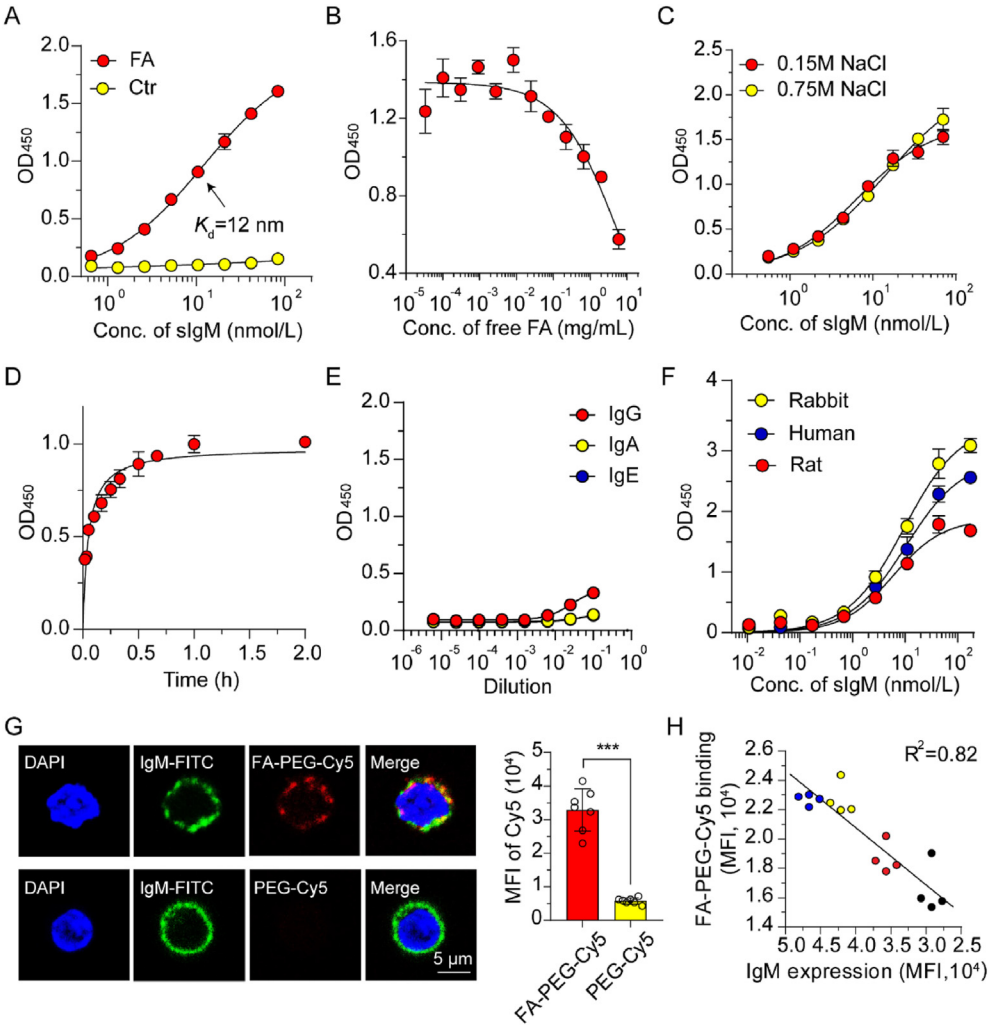

Figure 1 Specific binding of folic acid (FA) with IgM. (A) Direct binding of FA and sIgM from BALB/c mice. FA was immobilized on 96-well ELISA plates after conjugation with PEG-DSPE. mPEG-DSPE was used as a negative control. (B) Inhibition of free FA on the specific interaction between FA and sIgM from BALB/c mice. (C) The effect of high concentration of sodium chloride on interaction between FA and sIgM from BALB/c mice. (D) Binding kinetics between FA and sIgM from BALB/c mice. (E) FA binding with IgG, IgA and IgE from BALB/c mice. (F) The effect of sIgM origin on FA binding. (G) Representative confocal microscopic images and quantitative comparison by flow cytometry for binding of Cy5-labeled FA (red, FA-PEG-Cy5) with mouse splenic B lymphocytes and colocalization with mIgM (green). PEG-Cy5 was used as a negative control (without FA conjugation, $n = 7$). Scale bar = 5 μm. (H) Correlation between the expression level of mIgM and FA-PEG-Cy5 binding ($n = 4$). Data are means ± SD, $^{***}P < 0.001$ by Student's t-test.

modification degree of 23) was intravenously injected into the tail vein of BALB/c mice (see scheme in Fig. 3A). After three injections, blood was sampled on Day 21 for determination of anti-OVA antibodies. As expected, consecutive injections of OVA induced significant anti-OVA IgG and IgE antibodies (Fig. 3B and C). In a sharp contrast, covalent conjugation of FA led to immune escape of OVA with undetectable anti-OVA antibodies. Coadministration of free FA and OVA (FA + OVA) also reduced the titers of anti-OVA antibodies to some extent, but the immunological escaping effect was weaker than that of the covalent conjugate (FA-OVA).

To assess the memory of FA-OVA induced immune escape, all mice were rechallenged with OVA on Days 21, 28 and 35 (see Fig. 3A). The first OVA rechallenge did not cause significant hypothermia in mice immunized with FA-OVA (Fig. 3D). The second rechallenge on Day 28 slightly enhanced immune response against OVA, but did not cause significant reduction of body temperature of FA-OVA immunized mice (Fig. 3C and D). The third OVA rechallenge induced hypothermia in FA-OVA immunized mice due to high titration of anti-OVA antibodies, suggestive of rapid recovery of immunological functions of MZB. In contrast, each OVA rechallenge caused significant hypothermia and even death of the mice immunized with OVA due to production of the high levels of anti-OVA antibodies.

Immunohistochemical analysis was performed after OVA rechallenge on Day 21. OVA but not FA-OVA caused heavy IgG complex deposition in liver and kidney of the mice suffering severe anaphylactic shock or even death (Supporting Information Fig. S9). The results of H&E histological examination (Supporting Information Fig. S10) and blood test (Supporting Information Table S1) suggested high biosafety of FA-OVA.

Since FA is a widely consumed nutrition supplement for human, the immunological effect of orally administered FA was investigated. As illustrated in Supporting Information Fig. S11A,

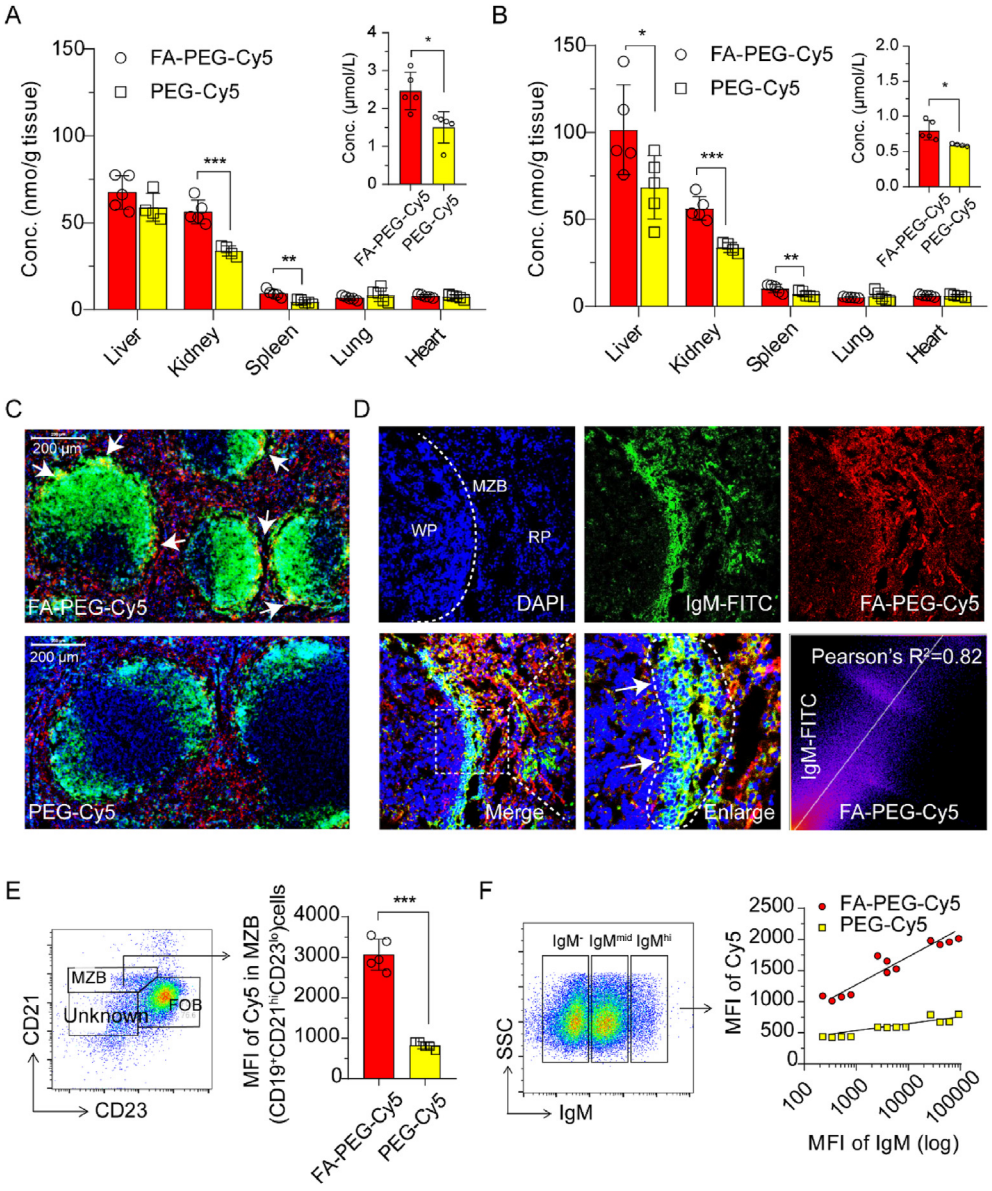

Figure 2 Marginal zone B (MZB) cells targeting of folic acid (FA) by binding with mIgM. Fluorescent dye Cy5 (red)-labeled FA (FA-PEG-Cy5) and the negative control PEG-Cy5 (without FA conjugation) were intravenously injected into BALB/c mice *via* the tail vein. Biodistribution of FA-PEG-Cy5 or PEG-Cy5 after 1 h (A) and 4 h (B) intravenous injection was quantified. Insert was the concentration of injectants in blood ($n = 4$). Data are means ± SD. $^*P < 0.05$, $^{**}P < 0.01$ and $^{***}P < 0.001$ by one-way ANOVA test. Immunofluorescence staining of spleen slices by anti-CD19 antibody for $CD19^+$ B lymphocytes (C, green) and anti-IgM antibody for IgM^{hi} MZB (D, green) at 1 h after injection. DAPI, blue. Arrows indicate colocalization of FA-PEG-Cy5 with MZB. Scale bar = 200 μm. (E) Statistical analyses of $Cy5^+$ MZB ($CD19^+CD21^{hi}CD23^-$) using flow cytometry at 1 h after injection ($n = 5$). (F) Correlation between the expression level of mIgM and uptake of FA-PEG-Cy5 by splenic B lymphocytes at 1 h after injection ($n = 4$). Data are means ± SD. $^{***}P < 0.001$ by Student's *t*-test.

BALB/c mice were intravenously immunized with OVA on Days 0, 7 and 14 accompanied with daily intragastric feeding of saline or free FA (3 mg/mouse). OVA induced a mounting antibody response as expected with each successive boost (the OVA group, Fig. S11B). Daily intragastric feeding of free FA during the whole immunization period (from the Days 0−14, the FA (i.g.) + OVA group) partially inhibited the anti-OVA response (detected on Day 21, a week after termination of OVA immunization and oral feeding with free FA). All mice were rechallenged with intravenous OVA on Days 21 and 28. The partial immune escape induced by oral FA was disappeared after the termination of daily feeding, leading to fully recovery of immunological response against OVA on Day 28. Free FA prevented IgE-induced anaphylactic shock. The body temperature maintained under normal condition after OVA challenge on Day 21, which decreased to some extent after the OVA rechallenge on Day 28 due to the disappearance of FA-induced immune escape (Supporting Information Fig. S11C).

3.4. Folic acid induces B cell anergy by destabilizing mIgM-BCR complex

As MZB cells shuttle between the marginal zone and follicles to deliver antigens rapidly from the open blood circulation[14], the expression levels of mIgM on MZB cells before and after OVA

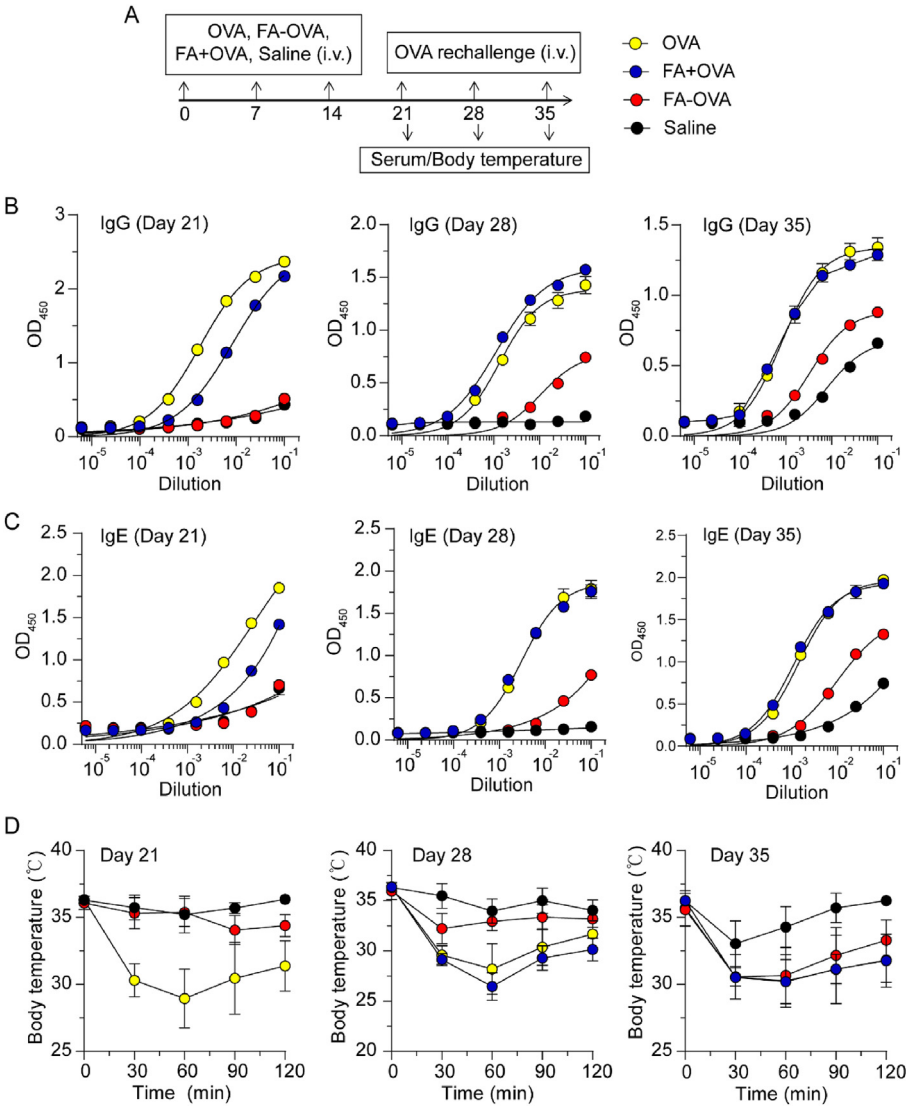

Figure 3 Reversible suppression the humoral immunity by folic acid (FA). (A) BALB/c mice were injected with FA conjugated ovalbumin (FA-OVA, 10 μg/mouse), OVA (10 μg/mouse), mixture of free FA and OVA (FA + OVA, 10 μg FA and 10 μg OVA/mouse) or saline *via* the tail vein on Days 0, 7 and 14. Animals were rechallenged with OVA (10 μg/mouse) on Days 21, 28 and 35. Body temperature was recorded and anti-OVA antibodies were determined using ELISA. Anti-OVA IgG (B) and IgE (C) on Days 21, 28 and 35. (D) Body temperature change of BALB/c mice after sequential OVA challenge on Days 21, 28 and 35. Data are mean ± SD. $n = 6-10$.

challenge were analyzed by immunofluorescence staining and flow cytometry (Fig. 4A and B). Consecutive OVA immunizations induced a significant decrease of mIgM expression. However, FA-OVA or the mixture of FA and OVA (FA + OVA) did not significantly alter mIgM expression on MZB cells in comparison to saline. On Day 21 before OVA rechallenge, mice were sacrificed to evaluate the maturation and differentiation of splenic B lymphocytes. OVA successfully activated the splenic B lymphocytes by expressing high levels of the proliferation marker CD86 and differentiation marker GL7 (Supporting Information Fig. S12). FA-OVA and FA + OVA failed to modulate the expression levels of CD86 and GL7, suggestive of the anergic-like status of splenic B lymphocytes after both FA treatments (FA-OVA and FA + OVA). Upon ligation with antigens, the heavy chains of mIgM are crosslinked with the heterodimer of the immunoglobulin α-chain (Igα) and immunoglobulin β-chain (Igβ) for signal transduction and antigen procession[22,23]. B lymphocytes are activated, proliferate, and differentiate into plasma cells for antibody production[24]. Deletion of the CH3 and CH4 domains of mIgM μ chain was verified to induce mIgM dissociation from the Igα/Igβ heterodimer[25]. As shown in Fig. 4C, free FA incubation for 1 h with splenic B lymphocytes induced approximate a decrease of 20% Igα and 28% Igβ in the coprecipitate, suggested that FA binding destabilized BCR to turn off B cell responses for anergy.

Cell lines expressing mIgM-BCR were utilized to further assess the association between FA-binding and mIgM-BCR stability. First, 293T cells were transfected with mIgM-BCR plasmids as illustrated in Fig. 4D. Western blot and flow cytometry showed that cell transfection led to the efficient expression of mIgM-BCR (Fig. 4E and F). Effective FA-binding with 293T cells expressing mIgM-BCR was observed after overnight incubation at

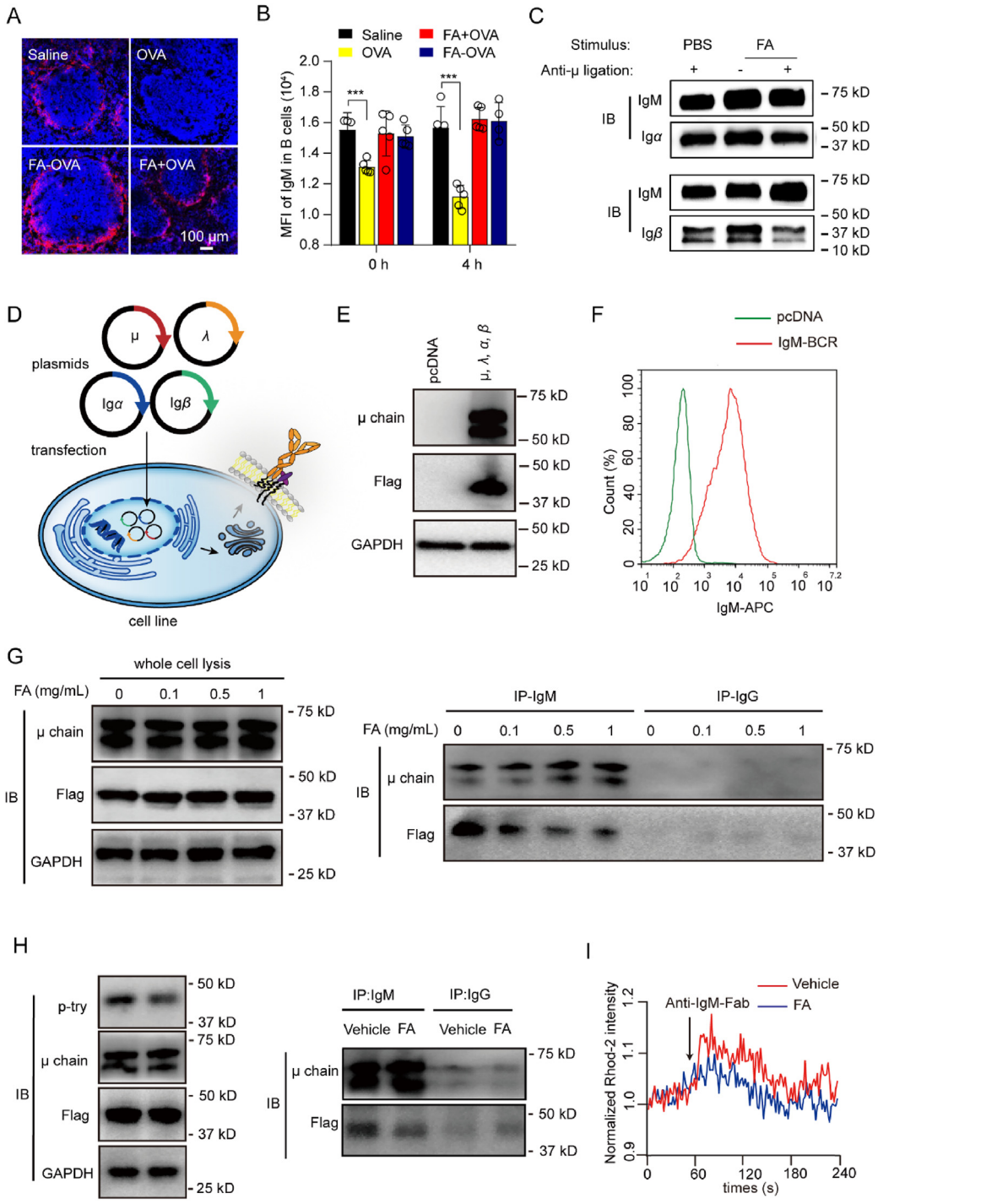

Figure 4 Folic acid (FA) induces B-cell anergy *via* destabilizing mIgM-BCR. mIgM expression in MZB cells by immunofluorescence staining (A) and flow cytometry (B). Spleen was harvested before (0 h) or 4 h after the first OVA challenge for cryosectioning. Nucleus (blue), mIgM (red). ***$P < 0.001$ by one-way ANOVA test, $n = 4$. Scale bar = 100 μm. (C) Comparative analysis of mIg-Igα/Igβ association. Splenic B lymphocytes were stimulated with FA for 1 h and sequentially ligated with anti-μ antibody for 5 min. Igα and Igβ immunoblots were detected after anti-μ immunoprecipitation. (D) Schematic illustration of establishing cell model expressing mIgM-BCR. 293T and A20 cells were transfected with mIgM-BCR expression plasmids (μ, λ, Igα, Igβ) or control empty vector (pcDNA). (E) At 48 h post-transfection, the expression level of plasmids of transfected-293T cells was detected by Western blotting with IgM μ and Flag Abs. GAPDH was used as control. (F) The expression level of mIgM-BCR of transfected-293T cells was measured by flow cytometry with staining anti-IgM-APC. (G) mIgM-BCR expressing 293T cell were incubated with FA at indicated concentration for 6 h. Whole cell lysates were separated by SDS-polyacrylamide gel electrophoresis and blotted for IgM μ chain and Flag. Simultaneously, lysates were immunoprecipitated with anti-IgM or anti-IgG and protein A/G agarose. mIgM-Igα/Igβ association was detected by blotting with anti-IgM μ, and anti-Flag. (H) mIgM-BCR expressing A20 cell were incubated with or without FA (1 mg/mL) for 6 h. Then A20 cells were stimulated by anti-IgM Fab (10 μg/mL) for 10 min. Whole cell lysates were separated by SDS-

4 °C (Supporting Information Fig. S13). We further examined the influence of FA on mIgM-BCR stability using transfected 293T cell. As show in Fig. 4G, the Co-IP experiments demonstrated FA binding with mIg heavy chain of mIgM-BCR decreased the ability of mIgM-BCR as FLAG (Igα/β) reduced in a dose-dependent manner. In addition, A20 B lymphoma cells (mIgG$^+$, mIgM$^-$, Supporting Information Fig. S14) were selected to further investigate whether FA-binding reduced the interaction of mIgM with Igα/β is functionally relevant. Similarly, A20 cells were transfected with mIgM-BCR plasmids and the expression of mIgM-BCR was verified by flow cytometry (Supporting Information Fig. S15). A significant feature of B cell activation is that phosphorylation of immunoreceptor tyrosine-based activation motifs (ITAMs) at the cytoplasmic domain of Igα/β initiate signaling transduction. Thus, we detected the level of protein tyrosine phosphorylation of A20 cells expressing mIgM-BCR stimulated by anti-IgM, and the level of protein tyrosine phosphorylation was increased in a time-dependent manner (Supporting Information Fig. S16). The level of phosphorylated Igα/β (p-Igα/β) in the absence or presence of FA in IgM-BCR expressing A20 B cells following anti-IgM Fab stimulation was further examined. The results indicated FA-binding suppressed phosphorylation of ITAMs (Fig. 4H), which reduced B cell activation signaling-transduction. mIgM-BCR stability was further assessed by immunoprecipitated, which was consistent with the data from mIgM-BCR transfected 293T cells (Fig. 4G). In addition, calcium flux signal was inhibited in the presence of FA in A20 cells expressing mIgM-BCR (Fig. 4I). In summary, these results suggested that FA-binding reduced mIgM-BCR stability within mIg heavy chain, which might induce B cell from activation to anergy.

The possible mechanisms of FA regulating function of mIgM-BCR in a structural level were further investigated *via* computational chemistry. We initially predicted the potential pockets allowing FA binding and identified two pockets which were located in Fab and Fc fragment respectively (Supporting Information Fig. S17). Given the topological size of FA, pocket located in Fc fragment was more suitable for accommodating FA molecules. Thus, we next obtained the computational complex of FA-mIgM with a docking score of −7.646 and the MM/GBSA ΔGbind energy of −44.39 kcal/mol, using molecular docking (Supporting Information Fig. S18). The docking pose was then submitted to molecular dynamics (MD) simulation to map potential allosteric process of mIgM with the binding of FA. From the snapshots, we could observe that FA always maintain stable interactions with mIgM by forming hydrogen bonds, but the conformation of mIgM at 100 ns was significantly different from that of 0 and 50 ns (Fig. 5A). We calculated the RMSD and radius of gyration to characterize the backbone change of mIgM at the whole dynamics. Results demonstrated that mIgM might experience two conformational changes at ∼40 and ∼70 ns respectively (Supporting Information Fig. S19). Data of RMSD and radius of gyration were then clustered to map the 2D free energy landscape which clearly showed the three metastable conformations that convert from S1 (0−30 ns) to S2 (50−70 ns) to S3 (80−100 ns) (Fig. 5B). We extracted the conformation of mIgM at 100 ns to form simulated complex with its downstream mIgα/β by using molecular docking. The topology and interactive mode of simulated complex was similar with the native cryo-EM structure of mIgM-mIgα/β (Fig. 5C and D). However, the binding free energy of simulated complex was dramatically weaker than that of cryo-EM structure (Fig. 5E). Binding free energy was further decomposed into individual residues, which showed that many contributions of residues were abolished in simulated complex (Supporting Information Fig. S20). From the results of computational chemistry, we can confer that FA could bind to the mIgM Fc fragment to induce conformational change and thus diminish the interaction with downstream mIgα/β for blocking signaling transduction.

3.5. *Folic acid alleviates the production of anti-drug antibodies (ADAs) of therapeutic biologics*

To investigate whether FA mitigates the production of ADAs, antibodies (adalimumab and infliximab) and proteins (interferon-α2b and hFVIII) drugs were selected due to their reported records of ADAs. FA was covalently conjugated to thiol groups in the Fc domain of antibodies (see Methods). As shown in Fig. 6A, FA-adalimumab significantly alleviated the adalimumab-specific antibody titers without altering its binding with recombinant human TNF-α (Fig. 6B) or pharmacokinetic profile in BALB/c mice (Fig. 6C). Infliximab- and interferon-α2b-specific antibody titers were also effectively suppressed after FA conjugation (Fig. 6D and E). Hemophilia A mice devoid of FVIII were used to mimic the development of neutralizing antibodies against recombinant hFVIII of severe hemophilia A patients. Administration of human coagulation factor hFVIII led to the production of neutralizing antibody, significantly impairing the procoagulant function to cause heavy blood loss of mice (Fig. 6F). In contrast, FA conjugation effectively reduced immunogenicity of hFVIII and the production of anti-FVIII antibody, preserving the procoagulant function of hFVIII after repeated administrations.

4. Discussion

Undesired immunogenicity caused by autoantigens, allergens and even therapeutic biologics have profound impact on human health[26,27]. Immunomodulatory agents, such as rapamycin, are commonly used to control immunogenicity. However, these immunosuppressive agents usually have broad immunosuppressive effects and require long-term administration, which may lead to infection, pathogens reactivation and tumor development[4,28]. Therefore, safe and effective immunomodulators need to be developed urgently.

Specific binding between sIgM and FA-enabled targeting vesicles in our previous work enlightened us to explore the interaction between FA and mIgM, as well as the consequent immunological effects. We are surprised to reveal that FA demonstrates immunosuppressive function by interfering with mIgM-BCR complex. Oral feeding or covalent conjugation of folic acid with therapeutic proteins and antibodies induces anergy of MZB cells to transiently escape immunological responses towards

polyacrylamide gel electrophoresis and blotted for total protein phospho-Igα/Igβ by mAb 4G10. Meanwhile, lysates were immunoprecipitated with anti-IgM μ and protein A/G agarose. The precipitates were immunoblotted with antibodies against Flag and IgM μ. (I) Ca^{2+} mobilization analysis of A20 cells expressing mIgM-BCR stimulated with anti-IgM Fab in the absence and presence of FA (1 mg/mL). Results are representative of at least three independent experiments.

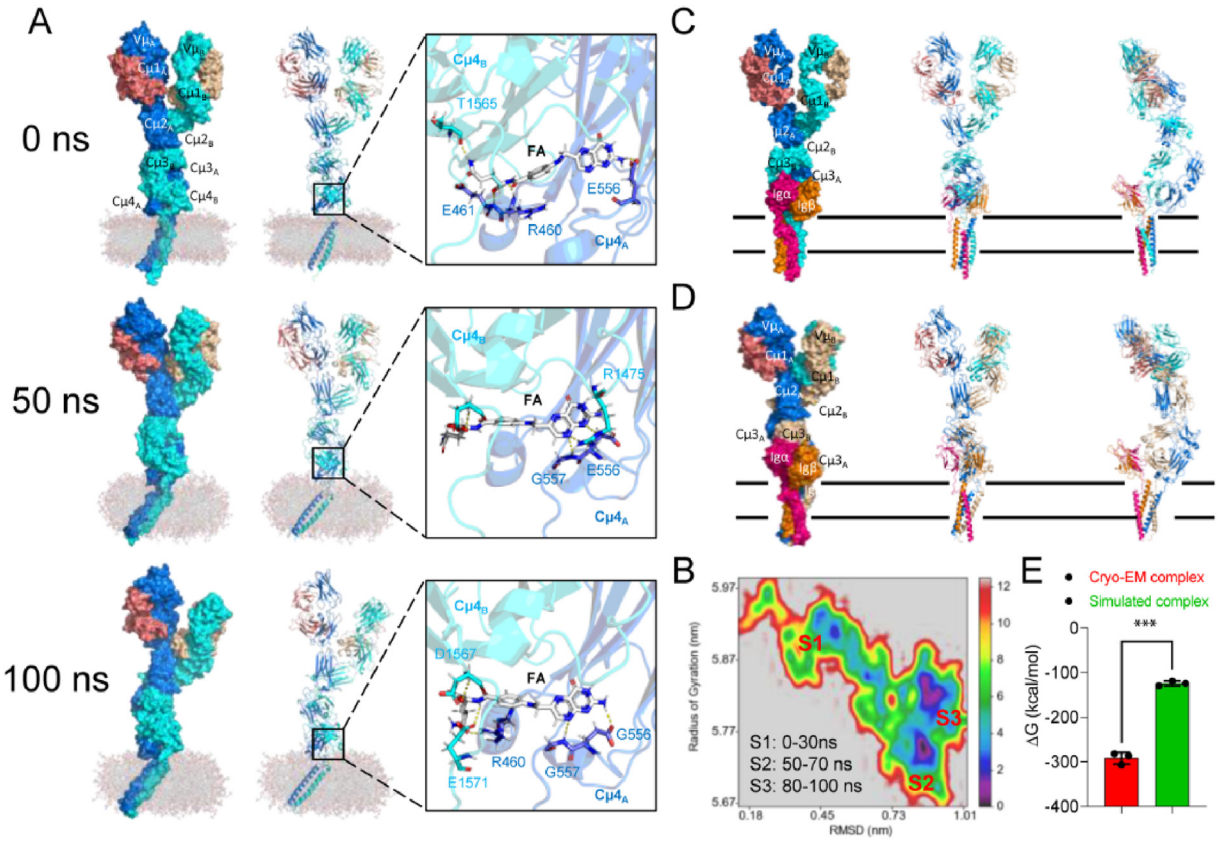

Figure 5 Folic acid (FA) binding induces conformational change of mIgM Fc fragment. (A) Snapshots of interaction between FA and mIgM sampling from all-atomic molecular dynamics simulation. (B) Free energy landscape of mIgM. (C) Cryo-EM structure of mIgM-mIgα/β complex. (D) Docking pose of conformation of mIgM extracted from MD trajectory at 100 ns with mIgα/β. (E) MM/GBSA binding free energy between mIgM and mIgα/β from native cryo-EM complex and docked pose.

antigens. FA at least partially mitigates the production of ADAs, which is a major obstacle to the long-term treatment of biologics by reducing curative effects and/or causing adverse reactions. FA acts as a safe and effective immunosuppressant to boost the clinical outcomes by inhibiting the production of ADAs, and also holds the potential to treat other indications that adverse immune responses need to be transiently shut off.

In the present work, FA conjugation was less effective to mitigate immunogenicity of the tested therapeutic biologics than that of OVA. OVA, with a molecular weight of 45 kDa, yielded an average conjugating ratio of 1:23 to FA. However, the therapeutic biologics acquired lower conjugating ratios than OVA (adalimumab 1:5.6; infliximab 1:3.6; and interferon α2b 1:1.5) due to their restrictions of the available modification sites. Although hFVIII yielded a higher conjugating ratio (1:34.8), it possesses a much larger size (300 kDa) than OVA. High FA conjugation ratio may be attributed to entire remission of anti-OVA antibodies after immunization with FA-OVA. Optimization of the FA conjugation, including conjugation ratio, site and linker, may dramatically expand the clinical application values.

In addition, these tested therapeutic biologics would possess more complicated antigen epitopes and immunogenicity (both T-dependent and T-independent mechanisms) than OVA. Splenectomy was performed to evaluate the contribution of spleen in the production of anti-adalimumab and anti-OVA antibodies. However, even though the absence of spleen, the production of adalimumab-specific antibodies remained significant regardless of injection routes (i.v. or i.c.), suggesting other APCs or immune organs contributed to the production of adalimumab-specific antibodies (Supporting Information Fig. S21A). In sharp contrast, undetectable anti-OVA antibodies were found after removal of spleen, indicating that spleen was the dominant organ for OVA immunization *via* blood (Supporting Information Fig. S21B). Our results discovered the immunosuppressive ability of FA for blood-borne antigens *via* splenic MZB-mediated immunization.

Oral FA is convenient for clinical application, but demonstrated lower effectiveness in mitigating the production of ADAs than covalent conjugation. Oral FA was ineffective for adalimumab but partially effective for the other tested antibody and protein drugs. Significant individual differences in the ADA titers were observed among mice after receiving oral free FA and therapeutic biologics (4/6 for infliximab, 3/6 for interferon-α2b and 2/4 for hFVIII were effective, Fig. 6D, E and F), which may be attributed to the individual difference of FA pharmacokinetic profiles. In addition, each B cell possesses up to 120,000 BCR complexes on its surface[29]. FA cannot block such abundant BCR due to its poor bioavailability which limit immunosuppressive function of FA. Although the non-memory and recoverable effect of folic acid restricts its application as potent long-term immunosuppressant like rapamycin, we demonstrated that the combination of FA effectively mitigated the production of ADAs, with a far-ranging function on monoclonal antibodies and recombinant proteins. Such effect might be meaningful to improve clinical outcomes of therapeutic biologics.

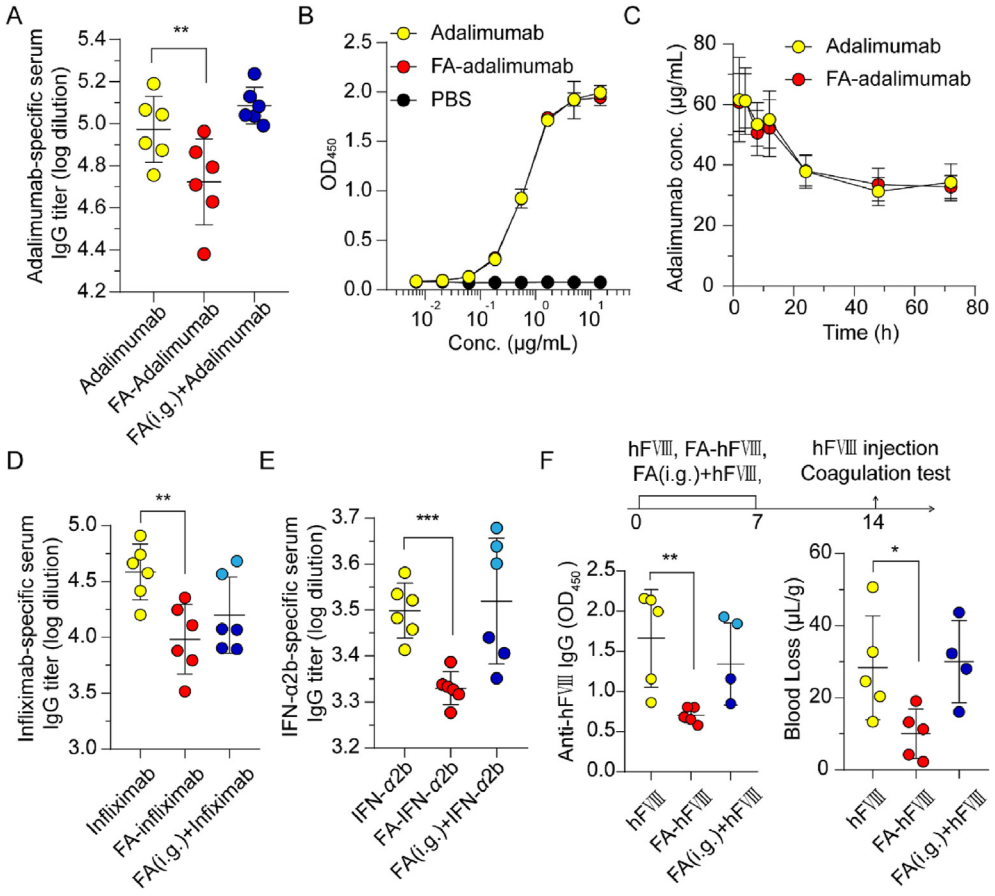

Figure 6 Folic acid (FA) mitigates the production of anti-drug antibodies. (A) Inhibition of anti-drug antibody response of adalimumab by FA-conjugation or oral FA. BALB/c mice were subcutaneously injected with FA conjugated adalimumab (FA-adalimumab), adalimumab, mixture of free FA and adalimumab (FA + adalimumab) or saline weekly for 8 weeks. For FA (i.g.) + adalimumab group, mice were intragastrically fed with 3 mg of FA daily and intravenously injected with adalimumab weekly for 8 weeks. Anti-adalimumab IgG in serum was measured one week after the last administration. Effect of FA on (B) binding of adalimumab with recombinant human TNF-α and (C) pharmacokinetic profile of adalimumab in BALB/c mice. (D) Anti-infliximab IgG titers. (E) Anti-IFN-α2b IgG titers. (F) Effects of FA on the production of anti-FVIII IgG and coagulation potency of hFVIII. FVIII KO hemophilia A mice were intravenously administered with hFVIII, FA conjugated hFVIII (FA-hFVIII), or saline on Days 0 and 7. For FA (i.g.) + hFVIII group, mice were intragastrically fed with 3 mg of FA daily and intravenously injected with hFVIII on Days 0 and 7. Anti-FVIII IgG was measured on Day 14. Coagulation test was conducted 1 h after intravenous administration with hFVIII of all mice on Day 14. Blood loss was recorded. Data are means ± SD, $n = 4-6$. $^*P < 0.05$, $^{**}P < 0.01$ and $^{***}P < 0.001$ by one-way ANOVA test.

5. Conclusions

In summary, FA was found to target MZB cells *in vivo* by binding mIgM with high affinity, destabilizing BCR to turn off B cell responses for anergy. FA acted as an immunosuppressant after covalent conjugation with therapeutic biologics to partially mitigate the production of anti-drug antibodies. The anergic state of MZB could also be induced by oral FA during the feeding period, which was rapidly recovered after the termination of feeding. However, the immunological escaping effect of oral FA on therapeutic biologics exhibited significant individual differences, which may be attributed to the absorption and pharmacokinetic profile of FA. Although both oral FA and FA conjugation need to be optimized to mitigate the production of ADAs, the present study paved a new avenue to improve clinical outcomes of therapeutic biologics by exploiting FA as a safe and effective immunosuppressant.

Acknowledgements

This work was supported by the National Natural Science Foundation of China (82125035, 81973245 and 82373817, China), and Shanghai Education Commission Major Project (2021-01-07-00-07-E00081, China). The author would like to thank Professors Weiyue Lu (School of pharmacy, Fudan University, China) and Wuyuan Lu (School of Basic Medical Sciences, Fudan University, China) for their insightful discussions.

Author contributions

Huan Wang, Zhuxuan Jiang and Zhiwei Guo performed most of the experiments and contributed equally to this work. Changyou Zhan conceived and designed the research. Gan Luo helped with the computational chemistry. Tianhao Ding helped with the

animal experiments. Huan Wang, Zhiwei Guo and Changyou Zhan analyzed the data and wrote the manuscript. All authors read and approved the manuscript. The patent concerning the technology presented in this work is applying for.

Conflicts of interest

The authors have no conflicts of interest to declare.

Appendix A. Supporting information

Supporting data to this article can be found online at https://doi.org/10.1016/j.apsb.2023.09.011.

References

1. Mullard A. 2020 FDA drug approvals. *Nat Rev Drug Discov* 2021;**20**:85−90.
2. Holdsworth SR, Gan PY, Kitching AR. Biologics for the treatment of autoimmune renal diseases. *Nat Rev Nephrol* 2016;**12**:217−31.
3. Zhang X, Hai L, Gao Y, Yu G, Sun Y. Lipid nanomaterials-based RNA therapy and cancer treatment. *Acta Pharm Sin B* 2023;**13**:903−15.
4. Sathish JG, Sethu S, Bielsky MC, de Haan L, French NS, Govindappa K, et al. Challenges and approaches for the development of safer immunomodulatory biologics. *Nat Rev Drug Discov* 2013;**12**:306−24.
5. van Schouwenburg PA, Rispens T, Wolbink GJ. Immunogenicity of anti-TNF biologic therapies for rheumatoid arthritis. *Nat Rev Rheumatol* 2013;**9**:164−72.
6. Kalden JR, Schulze-Koops H. Immunogenicity and loss of response to TNF inhibitors: implications for rheumatoid arthritis treatment. *Nat Rev Rheumatol* 2017;**13**:707−18.
7. Cerutti A, Cols M, Puga I. Marginal zone B cells: virtues of innate-like antibody-producing lymphocytes. *Nat Rev Immunol* 2013;**13**:118−32.
8. Tan C, Noviski M, Huizar J, Zikherman J. Self-reactivity on a spectrum: a sliding scale of peripheral B cell tolerance. *Immunol Rev* 2019;**292**:37−60.
9. Yarkoni Y, Getahun A, Cambier JC. Molecular underpinning of B-cell anergy. *Immunol Rev* 2010;**237**:249−63.
10. Tobón GJ, Izquierdo JH, Cañas CA. B lymphocytes: development, tolerance, and their role in autoimmunity-focus on systemic lupus erythematosus. *Autoimmune Dis* 2013;**2013**:1−17.
11. Cambier JC, Gauld SB, Merrell KT, Vilen BJ. B-cell anergy: from transgenic models to naturally occurring anergic B cells?. *Nat Rev Immunol* 2007;**7**:633−43.
12. Schamel WW, Reth M. Monomeric and oligomeric complexes of the B cell antigen receptor. *Immunity* 2000;**13**:5−14.
13. Martin F, Kearney JF. Marginal-zone B cells. *Nat Rev Immunol* 2002;**2**:323−35.
14. Arnon TI, Horton RM, Grigorova IL, Cyster JG. Visualization of splenic marginal zone B-cell shuttling and follicular B-cell egress. *Nature* 2013;**493**:684−8.
15. Wang H, Lin SQ, Wang SL, Jiang ZX, Ding TH, Wei XL, et al. Folic acid enables targeting delivery of lipodiscs by circumventing IgM-mediated opsonization. *Nano Lett* 2022;**22**:6516−22.
16. Moharil P, Wan Z, Pardeshi A, Li J, Huang H, Luo Z, et al. Engineering a folic acid-decorated ultrasmall gemcitabine nanocarrier for breast cancer therapy: dual targeting of tumor cells and tumor-associated macrophages. *Acta Pharm Sin B* 2022;**12**:1148−62.
17. Fernandez M, Javaid F, Chudasama V. Advances in targeting the folate receptor in the treatment/imaging of cancers. *Chem Sci* 2018;**9**:790−810.
18. Naumann RW, Coleman RL, Burger RA, Sausville EA, Kutarska E, Ghamande SA, et al. Precedent: a randomized phase II trial comparing vintafolide (EC145) and pegylated liposomal doxorubicin (PLD) in combination versus PLD alone in patients with platinum-resistant ovarian cancer. *J Clin Oncol* 2013;**31**:4400−8.
19. Wang H, Ding TH, Guan J, Liu X, Wang J, Jin PP, et al. Interrogation of folic acid-functionalized nanomedicines: the regulatory roles of plasma proteins reexamined. *ACS Nano* 2020;**14**:14779−89.
20. Ding TH, Guan J, Wang MK, Long QQ, Liu X, Qian J, et al. Natural IgM dominates *in vivo* performance of liposomes. *J Contr Release* 2020;**319**:371−81.
21. Yang J, Reth M. Oligomeric organization of the B-cell antigen receptor on resting cells. *Nature* 2010;**467**:465−9.
22. Dylke J, Lopes J, Dang-Lawson M, Machtaler S, Matsuuchi L. Role of the extracellular and transmembrane domain of Ig-α/β in assembly of the B cell antigen receptor (BCR). *Immunol Lett* 2007;**112**:47−57.
23. Shen ZX, Liu SC, Li XX, Wan ZP, Mao YX, Chen CL, et al. Conformational change within the extracellular domain of B cell receptor in B cell activation upon antigen binding. *Elife* 2019;**8**:e42271.
24. Noviski M, Mueller JL, Satterthwaite A, Garrett-Sinha LA, Brombacher F, Zikherman J. IgM and IgD B cell receptors differentially respond to endogenous antigens and control B cell fate. *Elife* 2018;**7**:e35074.
25. Tolar P, Hanna J, Krueger PD, Pierce SK. The constant region of the membrane immunoglobulin mediates B cell-receptor clustering and signaling in response to membrane antigens. *Immunity* 2009;**30**:44−55.
26. Gould HJ, Sutton BJ. IgE in allergy and asthma today. *Nat Rev Immunol* 2008;**8**:205−17.
27. Boehncke WH, Brembilla NC. Immunogenicity of biologic therapies: causes and consequences. *Expet Rev Clin Immunol* 2018;**14**:513−23.
28. Carbone J, Del Pozo N, Gallego A, Sarmiento E. Immunological risk factors for infection after immunosuppressive and biologic therapies. *Expert Rev Anti Infe Ther* 2011;**9**:405−13.
29. Yang JX, Reth M. The dissociation activation model of B cell antigen receptor triggering. *FEBS Lett* 2010;**584**:4872−7.